

Teaching a Master Student how to Model the Electrical Potentials Produced by the Muscle*

JAVIER RODRIGUEZ, JAVIER NAVALLAS and ARMANDO MALANDA

Department of Electrical and Electronic Engineering, Public University of Navarra, Campus de Arrosadía, 31006 Pamplona, Spain. E-mail: javier.rodriguez.falces@gmail.com

In Electromyography studies, the motor unit is considered as the anatomical and functional unit responsible of the electrical activity related to the contraction of the skeletal muscle. This paper is aimed at showing biomedical engineering master students how to model and study the electrical potentials produced by the activation of the motor unit. The proposed model is based on a mathematical concept familiar to engineers, the convolution. By using computer simulations based on this model, the effects of changes in the motor unit parameters on the characteristics of generated electrical signal are illustrated. The paper is useful in showing the students how to identify the different aspects involved in the analysis of biological phenomena.

Keywords: motor unit; muscle fiber; computer simulation; single fiber action potential (SFAP); motor unit action potential (MUAP)

1. INTRODUCTION

BIOMEDICAL ENGINEERING, as defined by the Whitaker Foundation [1], is a discipline that advances knowledge in engineering, biology and medicine, and improves human health through cross-disciplinary activities that integrate the engineering sciences with the biomedical sciences and clinical practice. As early as 1975, the *IEEE Transactions on Biomedical Engineering* published a special issue that discussed many of the challenges pertaining to biomedical engineering [2–6]. Since these early years, a number of authors [7–13] have reported a steady growth in biomedical engineering, showing that it has gained ‘acceptance as body of knowledge soundly based in both the biomedical and engineering disciplines’. Following this trend, Higher Education in Spain has given priority to the development of studies in the fields of Biomedicine and Biomedical Engineering.

The Public University of Navarra (Spain) is relatively young (it was established in 1987) so that it has shown itself to be very dynamic in incorporating changes, and this new environment is no exception. In an attempt to adapt to this framework, our university has promoted the creation of the Master’s Program of Biomedical Engineering (BME) since 2007. Our Master Degree in BME encompasses most of the key areas suggested by the Whitaker Foundation for the BME curriculum [14], such as Biomechanics, Bioinstrumentation, Biosystems, Computational Biology or Bioimaging.

One of the main subjects treated in the master is Bioelectricity. Indeed, electricity is the cornerstone of the Biomedical Engineering studies as it is essential for the understanding and interpretation of many biological processes [15]. Present work is aimed at showing BME master students how to model and study the electrical behaviour of a well-known biological system: the motor unit. In Electromyography studies, the motor unit represents the functional unit of a skeletal muscle that controls both its electrical activity and contraction mechanism [16, 17]. Our approach contains several aspects of relevance to the biomedical engineer’s background:

- 1) it identifies the anatomical, physiological and functional properties of the biological system under study;
- 2) it shows how to develop a mathematical model that comprises the abovementioned system properties;
- 3) it emphasizes the importance of the recording conditions on the generated electrical signal;
- 4) it illustrates how to analyse the effects of changes in the system properties on the generated electrical signal.

It is generally accepted that students learn an engineering topic best when they see the physical results of the experiments they perform [14, 18, 19]. However, this is not always possible when dealing with a biological system such as the motor unit. In this particular case, recording of the electrical signals is carried out by a specialist physician using a needle electrode that is inserted into the muscle, which produces a certain degree of pain to

* Accepted 21 June 2010

the subject [20]. Such tests cannot be performed by the students and this leads teachers to look for educational alternatives such as the use of computers to model and simulate biological processes. Indeed, computer simulation becomes an invaluable tool in teaching the structure and functioning of the motor unit.

Classical approaches to model the electrical behavior of the motor unit [21–25] presented important limitations as a pedagogical tool:

- 1) they normally comprised complex mathematical formulation which makes them somewhat unsuitable for teaching purposes;
- 2) they were not intuitive as they were more focused on the investigation;
- 3) they were not computationally efficient and were therefore highly time-consuming.

To circumvent these limitations, we proposed a model based on a mathematical concept familiar to engineers; the convolution [26, 27].

In the course of Bioelectricity, simulations were carried out using MATLAB, i.e. a software package available for desktop PCs, which has already been used by other authors as a pedagogical tool [28–30]. Specifically, the authors have developed a set of simulation programs on MATLAB in order to allow the students:

- 1) to obtain a better understanding of the generation of electrical potentials produced by the muscle contraction;
- 2) to appreciate how the changes in the motor unit parameters affect the properties of the generated electrical potentials.

It has been the belief of the authors that an electrical model of the motor unit together with a carefully designed collection of simulation programs based on this model contribute to a

more solid and well-founded background of the biomedical engineer.

2. STRUCTURE AND FUNCTIONING OF THE MOTOR UNIT

A muscle creates a desired level of force via the repeated contraction of a number of groups of muscle fibers. Each group of muscle fibers is controlled by an alpha-motor neuron [16]. Specifically, the motoneuron governs simultaneously a group of muscle fibers that are attached to its axon terminal branches at the neuromuscular junctions (NMJ) (Fig. 1). The motor unit (MU) is the system formed by a single motoneuron (the axon belongs to it) and all the muscle fibers that it innervates, and represents the anatomic and functional unit of a skeletal muscle (Fig. 1) [31]. The end-plate of a motor unit is the region where the neuromuscular junctions of its fibers are located [17].

Each individual skeletal muscle is activated by electrical impulses coming from the motoneuron through its axon. When an electrical impulse arrives at the neuromuscular junction it is converted into two intracellular action potentials (IAPs) that propagate in opposite directions along the muscle fiber towards the left and right tendons where they terminate (Fig. 1) [22]. The propagation of the IAPs along the muscle fiber generates an electrical potential in the extracellular medium, the so-called single fiber action potential (SFAP), that can be recorded by an electrode [23]. The superposition in time and space of the SFAPs from all the muscle fibers of a single motor unit is the motor unit action potential (MUAP).

The structure and functioning of the motor unit is described in Fig. 1. For the students to obtain more insight into the architecture of the muscle it is necessary to provide further information on how

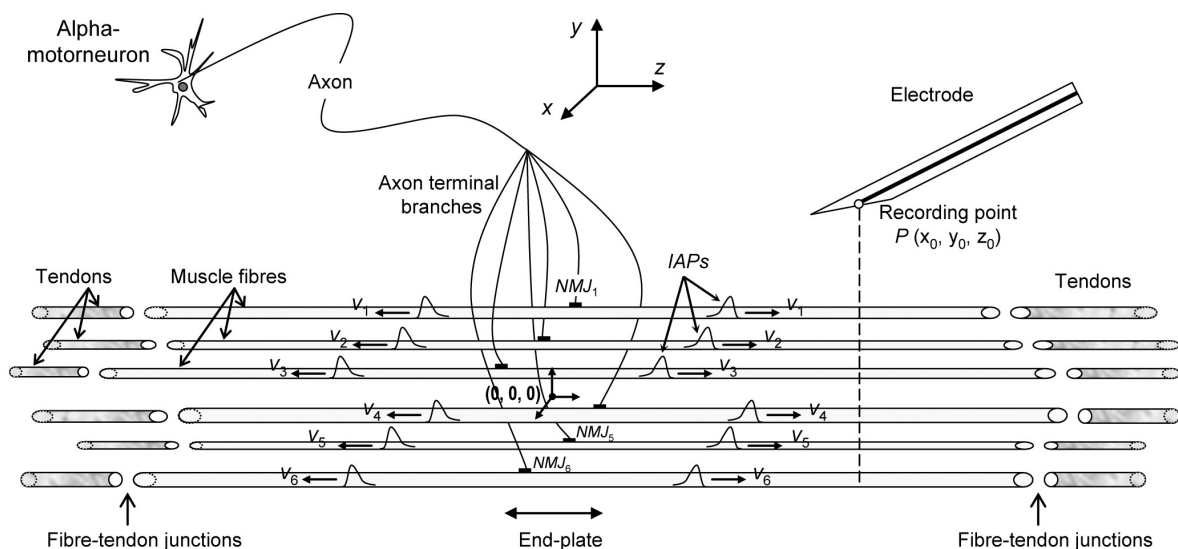


Fig. 1. Schematic representation of the elements of a motor unit.

the motor unit is integrated within the muscle. The different views of the muscle represented in Fig. 2 help the student to establish a solid framework, appropriate for developing their intuition. The following aspects are highlighted in Fig. 2:

- 1) The muscle cross-section in which the fibers of a MU are distributed is called *MU territory*. It is important to emphasize that the MU territories of several MUs may overlap as the muscle fibers of one MU are not compactly packed, but are mixed with the fibers of other MUs in the global muscle mass [Fig. 2(a)] [16].
- 2) In Fig. 2(b) we show a cross-section of the whole muscle, where the territory of the MUs depicted on the left appears within a small rectangle. In doing so, students can appreciate the relative dimension of the MU territory as compared to the muscle size.
- 3) Fig. 2(c) represents the muscle longitudinal section where the positions of the end-plate and tendons are indicated. The muscle fibers corresponding to MUs depicted in Fig. 2(a)

can be recognized easily as they have been plotted using thicker lines than the other fibers.

In each diagram of Fig. 2, the electrode, fibers, MU territory and muscle have been drawn approximately to scale using the dimensions of a normal biceps brachii muscle as a reference [32]. Therefore, these diagrams allow the comparison of the size of the electrode with that of the fiber diameter, fiber length, MU size, and muscle diameter.

Based on the authors' teaching experience, students tend to think they fully understand the space dimensions of the muscle architecture as soon as they are shown the motor unit picture, depicted in Fig. 1. However, the three dimensions of the problem are barely represented in this picture and students often feel puzzled when they must identify these three dimensions in the three diagrams shown in Fig. 2. The detail of the motor units, together with the cross- and longitudinal sections of the muscle and their corresponding axis are essential to understand correctly the generation of extracellular electrical potentials.

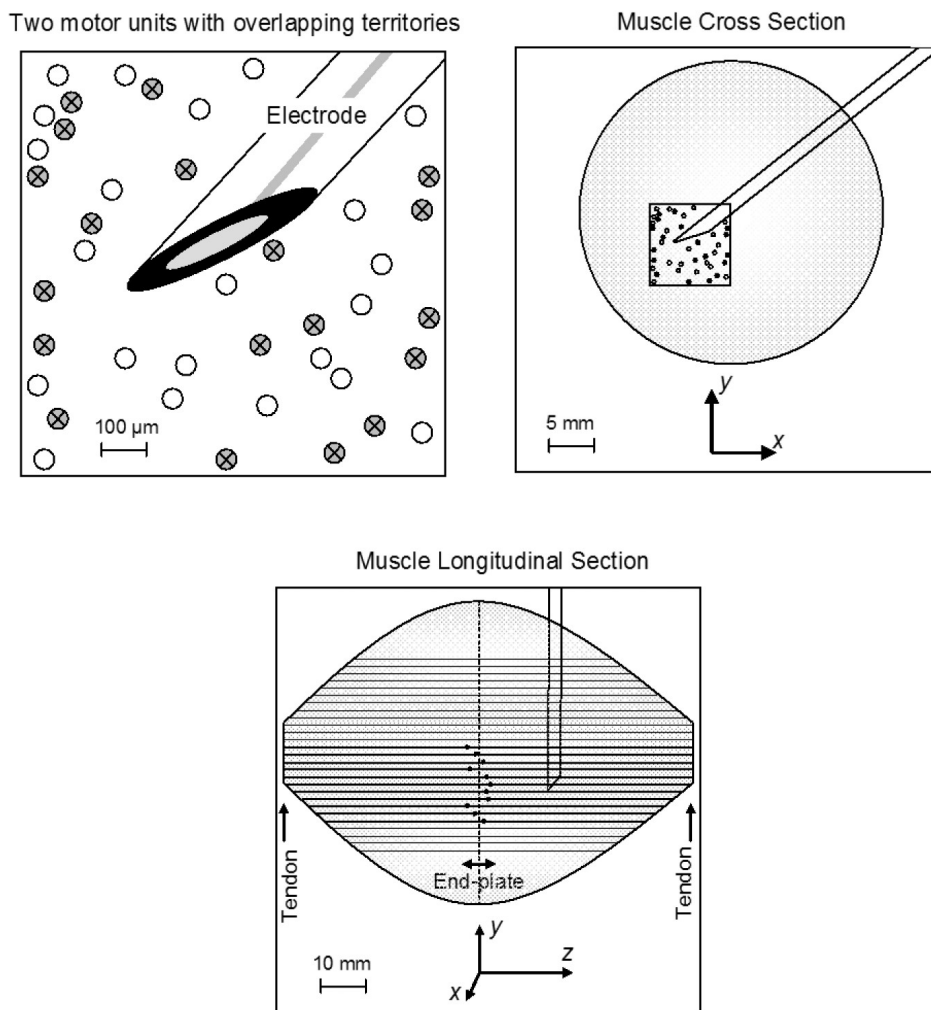


Fig. 2. (a) Muscle fibers (empty and crossed circles) of two different motor units. Cross-section (b) and longitudinal section (c) of a normal biceps brachii muscle.

3. MODELLING SINGLE FIBER ACTION POTENTIALS (SFAPS) AND MOTOR UNIT ACTION POTENTIALS (MUAPS)

The next step is to show the students how to model mathematically the structure and functioning of the motor unit. As expected, the mathematical descriptions of SFAPs and MUAPs are based on a number of simplifications. By assuming that the shape of the IAP and the propagation velocity are practically not altered along the fiber (which is a reasonable assumption based on [33–35]), the skeletal muscle fiber of finite length can be considered as a linear and time-shift invariant system [26]. Under these conditions, the potential generated by a single fiber (SFAP) can be expressed as a convolution of the input signal and impulse response (*IR*) of the corresponding system [26, 27, 36]:

$$SFAP(t) = C \cdot d^2 \cdot \frac{\partial^2 IAP(t)}{\partial t^2} * IR(t) \quad (1)$$

where *C* is a coefficient of proportionality that depends on the tissue conductivity (with a typical value of $0.02 \text{ ms} \cdot \text{mm}^{-1}$) and *d* is the fiber diameter (in mm). The input signal is the second temporal derivative of the intracellular action potential, $\partial^2 IAP(t)/\partial t^2$. One of the most used analytical functions for IAP is [27]:

$$IAP(t) = 96t^3 e^{-2t} \quad (2)$$

In (1), the impulse response (*IR*) is computed as

$$IR(t) = \frac{1}{\left[(z_0 - NMJ - vt_1)^2 + r^2 \right]^{\frac{1}{2}}} + \frac{1}{\left[(z_0 - NMJ + vt_2)^2 + r^2 \right]^{\frac{1}{2}}}, \quad t_1 \in \left[0, \frac{L_1}{v} \right], \quad t_2 \in \left[0, \frac{L_2}{v} \right] \quad (3)$$

In (3), the first and second terms at the right side of the equation correspond to the potentials produced at the recording point by the IAP propagating along the fiber from the end-plate to the right tendon and to the left tendon, respectively. In view of Eq. (3), the students should realize that the propagation of the IAP in the opposite directions is symmetrical. In the definition of the *IR* it is important to notice that the origin of coordinates is assumed to be located at the geometric centre of the muscle. All the variables appearing in (3) are shown in Fig. 3(a). Specifically, the impulse response comprises:

- Anatomical properties of the fiber: right semilength, L_1 (in mm), left semilength, L_2 (in mm), and neuromuscular junction position, *NMJ* (in mm), with respect to the coordinate origin.
- Physiological properties of the fiber: propagation velocity, *v* (in mm/ms).

- Detection conditions: fiber-to-electrode distance, *r* (in mm), longitudinal position of the electrode with respect to the coordinate origin, z_0 (in mm).
- Duration properties: t_1 and t_2 (in ms) represent the time elapsed between the onset of IAP at the NMJ and its termination at the right and left fiber-tendon junctions, respectively.

The propagation velocity and fiber diameter are assumed to have a linear relationship [27] given by

$$v(m/s) = 4 + 0.05 \cdot (d - 0.055) \quad (4)$$

The radial distance (*r*) in (3) that can be calculated as

$$r = \sqrt{(x_0 - x_j)^2 + (y_0 - y_j)^2} \quad (5)$$

where (x_0, y_0) and (x_j, y_j) are the coordinates of the electrode and the muscle fiber, respectively. Looking at equation (5), students should realize that the radial distance is the minimum distance from the electrode to a certain fiber [calculated within the muscle cross section $z = z_0$, as shown in Fig. 3(a)].

If the physiological properties of the fiber are the same for all fibers of the MU, the IAP in time domain could be accepted as identical, irrespective of the fiber diameter [34, 35]. Then, the MU could also be considered as a linear time shift-invariant system, whose common impulse response (*CIR*) is the sum of *N* impulse responses corresponding to individual muscle fibers:

$$CIR(t) = \sum_{i=1}^{i=N} IR_i(t) \quad (6)$$

Instead of *N* convolutions (one for every fiber), the MUAP, as the output signal, can be calculated as a single convolution between the IAP second temporal derivative and the *CIR*:

$$MUAP(t) = C \cdot d^2 \cdot \frac{\partial^2 IAP(t)}{\partial t^2} * CIR(t) \quad (7)$$

In most cases the students found the equations and formulae clear and applicable, and therefore they were capable of understanding the corresponding programs implemented in MATLAB. Using this software package, the authors designed a set of simulation programs (see Appendix for details) that enable the students to feel the influence of the motor unit parameters on the amplitude and duration properties of the extracellular electrical potentials (SFAPs and/or MUAPs) generated by the activation of the motor unit.

4. STUDY OF THE AMPLITUDE-RELATED CHARACTERISTICS OF EXTRACELLULAR ELECTRICAL POTENTIALS

We will start using the models, shown in equations from (1) to (7), to illustrate how the electrode

position and the physiological properties of the fiber affect the amplitude characteristics of extracellular potentials. For the sake of clarity, students are advised to consider a scenario with only one muscle fiber and therefore to use the SFAP model (1). In this simplified scenario, they will analyze the effect of changes in r , z_0 and d on the amplitude of the recorded SFAP (see Fig. 3).

4.1 Impulse response parameters

As only one muscle fiber is considered, we can make it coincide with the origin of coordinates so that $x_j = y_j = 0$. Moreover, we can assume that this origin is located just at the position of the NMJ. It is important that students understand the implications of these simplifications in the diagram of Fig. 3(a). The default values used for the parameters of the muscle fiber, together with the ranges of variation considered in each of the simulations, are summarized in Table 1. The data shown in Table 1 represent real values that were obtained from a normal biceps brachii muscle [32].

4.2 Effects of varying radial distance

Students are told to increase r from 0.05 to 0.15 mm, while keeping the other MU parameters unchanged. As shown in Fig. 3(b), they should observe an abrupt decline of the SFAP amplitude when the electrode is moved further away from the fiber. This should not be surprising as Eq. (3) predicts a decrement in the voltage of the EMG signal with increasing r .

4.3 Effects of varying electrode longitudinal distance

The next task is to illustrate the influence of the longitudinal position of the recording point (z_0) on the SFAP amplitude. Students are advised to change z_0 from 0 to 40 mm in steps of 10 mm. They should notice that, when the electrode is sufficiently far from the end-plate and from fiber-tendon junction, the amplitude of SFAPs is independent of z_0 , and their waveforms have three phases [Fig. 3(c)]. However, if the electrode is just above the endplate ($z_0 = 0$ mm) and/or

Table 1 Parameter values of one muscle fiber of the biceps brachii in different simulations

	L_1 (mm)	L_2 (mm)	NMJ (mm)	d (mm)	z_0 (mm)	r (mm)
Varying r	40	50	0	0.055	20	0.05–0.15 (step of 0.05)
Varying z_0	40	50	0	0.055	0–40 (step of 10)	0.10
Varying d	40	50	0	0.025–0.065 (step of 0.020)	20	0.10

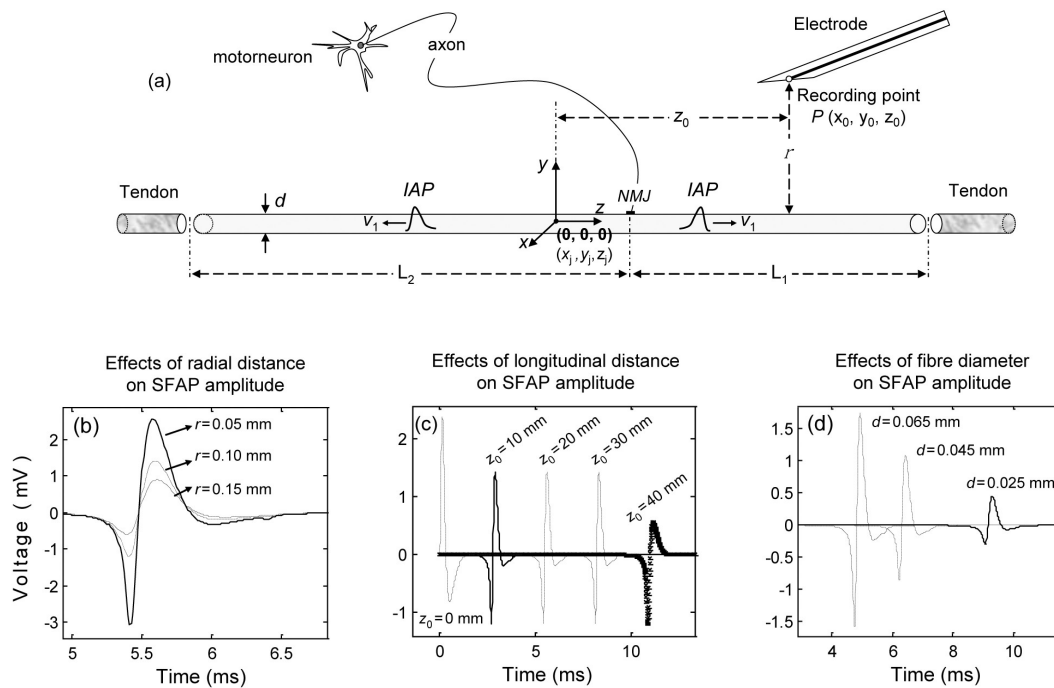


Fig. 3. (a) Schematic representation of a muscle fiber innervated by the axon of a motorneuron. Effects of changes of the radial distance of the electrode (b), longitudinal position of the electrode (c), and diameter of the fiber (d) on the amplitude of SFAPs.

above the fiber-tendon junction ($z_0 = 40$ mm), the SFAP amplitude changes significantly and the SFAP becomes biphasic [Fig. 3(c)].

4.4 Effects of varying fiber diameter

The effects of a varying fiber diameter can be easily predicted from Eq. (1), where d^2 is shown to act as a scale factor. Thus, an increase in d should be followed by an increase in the amplitude of the SFAP, as shown in Fig. 3(d). This figure also reveals that differences in the fiber diameter give rise to different latencies (or delays) of the corresponding potentials. The explanation for this lies in the fact that changes in d not only have an influence on the SFAP amplitude, but also affect the propagation velocity of the IAP along the fiber, as established in (4). According to this equation, a high value of d (0.065 mm) will allow the IAP to travel very fast ($v = 4.2$ mm/ms), reaching electrode longitudinal position in a short time [approximately 4.7 ms, as shown in Fig. 3(d)]. In contrast, a low value of d (0.025 mm) will make the IAP propagate slower ($v = 2.2$ mm/ms), which will delay its arrival to the electrode longitudinal position [approximately 9 ms, see Fig. 3(d)].

The differences in the propagating velocities between the fibers will give rise to time dispersion between the corresponding SFAPs which, in turn, will influence the shape of the resulting MUAP. Further details of the time summation of individual SFAPs are provided in the next section.

5. STUDY OF THE TIME-RELATED CHARACTERISTICS OF EXTRACELLULAR ELECTRICAL POTENTIALS

When a scenario with various muscle fibers is considered, such as that represented in Fig. 1, the students should realize that, at a certain instant of time, the longitudinal positions of the IAPs in the different fibers are not exactly the same; rather, the IAPs of different fibers are dispersed temporally due to a number of factors:

- Differences in length of the axon terminal branches.
- Scattering of the neuromuscular junctions within the end-plate.

- Differences in the propagation velocity of the different fibers.

In order to illustrate the effect of the time dispersion of various SFAPs belonging to different muscle fibers on the shape of the summated potential, we will consider the two scenarios shown in Fig. 4. As can be seen, each scenario comprises two muscle fibers whose characteristics are summarized in Table 2.

In scenario (a), the time dispersion is generated only by the difference in the positions of the neuromuscular junctions (NMJ) of fiber1 (0 mm) and fiber2 (1.5 mm). With the two fibers having the same propagation velocities ($v_1 = v_2$), SFAP2 arrives at z_{10} earlier than SFAP1 because its neuromuscular junction is closer to the right tendon. In this situation, SFAP2 is said to have lower latency than SFAP1. Moreover, since $v_1 = v_2$, the latency difference between SFAP1 and SFAP2 is the same at different longitudinal positions of the electrode. This explains why the sum of potentials SFAP1 and SFAP2 is the same at z_{10} and at z_{30} .

In scenario (b), the time dispersion is generated by the difference in both the neuromuscular junction positions and propagation velocities of fiber1 and fiber2. Specifically, the neuromuscular junction of fiber 2 is closer to the right tendon than that of fiber 1, and $v_2 > v_1$. In these conditions, the latency of SFAP1 is greater than that of SFAP2 and, more importantly, the latency difference between them increases as they spend more time propagating; i.e. as they approximate to the tendons. This can be appreciated in Fig. 4, where SFAP1 and SFAP2 clearly overlap at z_{10} , whereas they are completely separated at z_{30} .

6. STATISTICAL DISTRIBUTIONS TO MODEL REALISTIC MOTOR UNIT POTENTIALS

The motor unit is a good example to emphasize for the students the importance of using statistical distributions to model the inherent variability of biological structures. Since the motor unit action potential (MUAP) is the superposition in time and space of the SFAPs from all the muscle fibers of a certain motor unit, then the shape of a MUAP will

Table 2. Parameter values of two muscle fibers of the biceps brachii associated with two different scenarios

	L_1 (mm)	L_2 (mm)	NMJ_1 (mm)	NMJ_2 (mm)	d_1 (mm)	d_2 (mm)	z_{10} (mm)	z_{30} (mm)	r (mm)
Scenario (a)	40	50	0	1.5	0.055 ($v_1 = 3.7$ mm/ms)	0.055 ($v_2 = 3.7$ mm/ms)	10	30	0.17
Scenario (b)	40	50	0	1.5	0.045 ($v_1 = 3.2$ mm/ms)	0.055 ($v_2 = 3.7$ mm/ms)	10	30	0.17

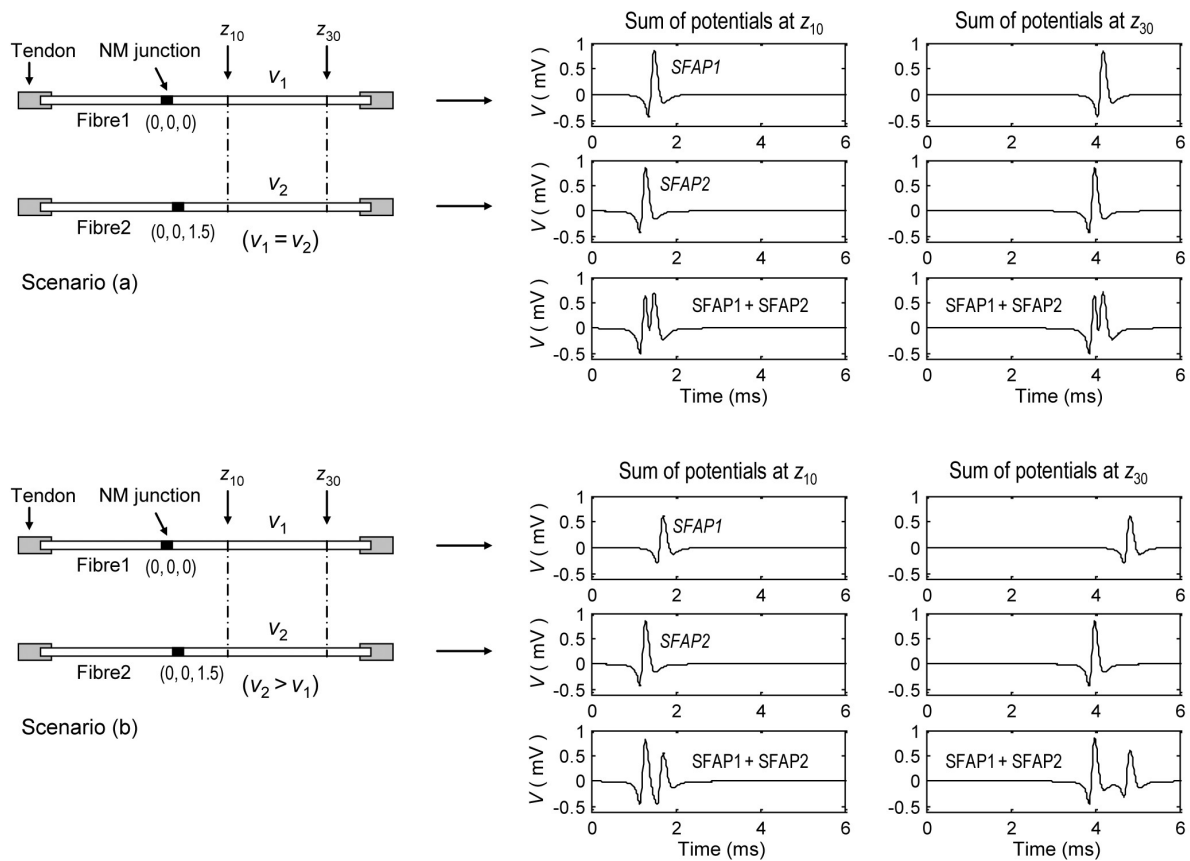


Fig. 4. Upper panel—schematic representation of two muscle fibers with identical properties but different NMJ positions (left) and their corresponding SFAPs recorded at $z_0 = 10$ mm and $z_0 = 30$ mm (right). Lower panel—the same as in the upper panel but with the muscle fibers having different propagation velocities.

be highly determined by the statistical distribution of the velocities and NMJ positions of the fibers belonging to that motor unit. More specifically, a realistic approach for the motor unit would require statistical distributions to model the variability in the following elements:

1. Diameters: in general, scientists assume that fiber diameters follow a Gaussian distribution (0.055 ± 0.0025 mm) ($M \pm SD$) [27, 37]. Since the propagation velocity is linearly related with the fiber diameter, the statistical distribution of v is indirectly determined by that of d .
2. End-plate: the Gaussian distribution (0 ± 0.5 mm) ($M \pm SD$) is normally used to model the variability in the positions of the neuromuscular junctions within the endplate of a motor unit [37].
3. Fiber lengths (and semilengths): the variability in the lengths of the different fibers can be assumed to have a Gaussian distribution: right semilength (40 ± 2 mm) and left semilength (50 ± 2 mm).
4. Fiber position within the motor unit: in a cross-section of the muscle, as that shown in Fig. 2(b), the fibers belonging to a certain motor units are considered to fall into circles of a diameter of about 10 mm. Within these

circles, fibers are distributed according to a uniform distribution [38].

By considering these statistical distributions and using Eq. (7), we simulate the MUAP shown in Fig. 5(a). This MUAP is recorded at a radial distance of 0.1 mm and at a longitudinal position of 20 mm. By taking this MUAP as a reference, we will introduce controlled variation in each of the MU statistical distributions, leaving the other ones unchanged. In doing so, students will be able to appreciate the sensitivity of the MUAP waveform to the changes in each distribution.

The MUAPs shown in Figs. 5(b) and (c) are obtained using the same statistical distributions as for the reference MUAP, but with an increase in the dispersion of d (and therefore in the variability of v). As the difference in the conduction velocities between the different fibers increases, the time dispersion of their corresponding SFAPs becomes higher, resulting in a longer and more complex MUAP. Students should note that the number of turns (peaks in the waveform) in the MUAPs of Fig. 5(b) and (c) is clearly higher than in the reference MUAP.

The MUAPs shown in Figs. 5(d) and (e) are simulated using the same distributions as for the reference MUAP, but with an increase in the

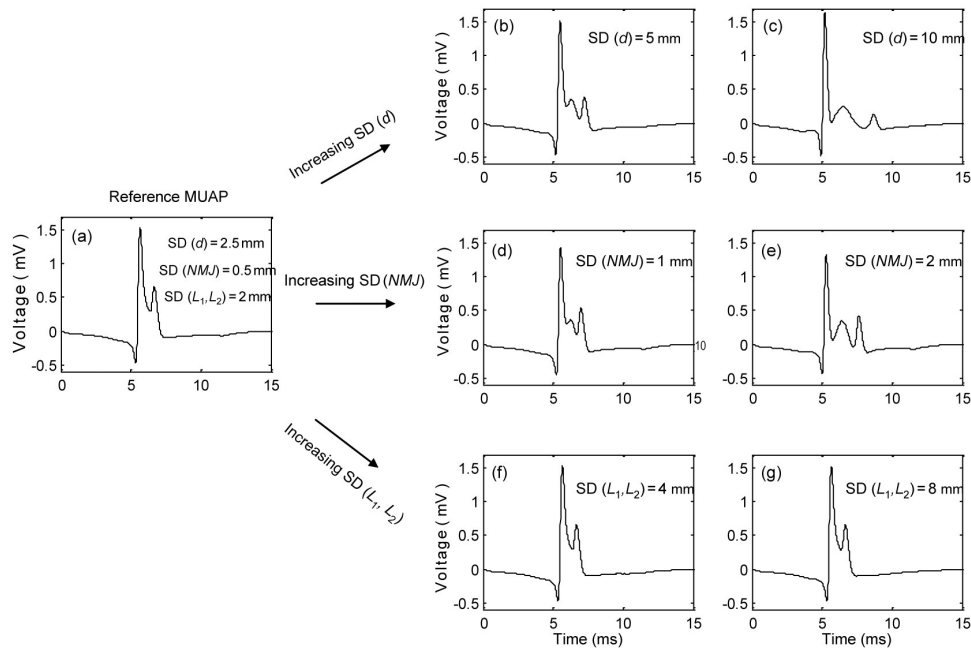


Fig. 5. Simulation of various motor unit action potentials (MUAPs) using different values for the statistical distributions of the fiber diameter (d), neuromuscular junction (NMJ) and right (L_1) and left (L_2) fiber semilengths.

dispersion of the NMJ positions. The widening of the end-plate region also results in higher time dispersion between individual SFAPs, increasing the duration and complexity of the MUAPs. By comparing Fig. 5(d) and (e), the students should appreciate that the three positive peaks of the MUAPs are better distinguished when the end-plate region is wider [higher $SD(NMJ)$].

By increasing the dispersion of both the left and right fiber semilengths, we obtain the MUAPs shown in Figs. 5(f) and (g). The students should note that, as compared to the reference MUAP, the shape of the MUAPs' main spike is practically unchanged. This is due to the fact that the MUAPs are recorded at a longitudinal position of 20 mm; i.e. sufficiently far from the fiber-tendon junctions.

7. DISCUSSION

6.1 Innovative contribution of the SFAP convolutional model

Lorente de Nó [21] was the first to obtain an expression for the potential of the external field of a nerve in a volume conductor as a function of an action potential. After his pioneering work, some other authors [22–25] derived new formulations to calculate the extracellular potential produced by an excitable fiber. However, these approximations are mathematically complex and therefore have a limited value as a pedagogical tool. Moreover, the fact that they are all designed to model bioelectrical phenomena as accurately as possible makes them time consuming, less intuitive and somewhat unsuitable for teaching purposes.

It was not until 1983 that Nandekar and Stål-

berg [27] proposed an easy description of the extracellular potential based on a convolution between an excitation function and a weight function. This description was further improved in 1998 by Dimitrov and Dimitrova [26] who, on the basis of previous works [39, 40], considered the muscle fiber as a timeshift-invariant system for SFAP generation. The presentation of the SFAP as a convolution between an input signal and an impulse response is appropriate for biomedical engineering students who are familiarized with this type of models. Another big advantage of this presentation is that it affords the possibility of making independent changes in the excitation and impulse response functions. This allows the separation of the parameters related to the volume conductor (included in the IR) from those related to the source of excitation, i.e. the IAP. This flexibility enables study of the effect of the model's parameters on the waveform of the potential, providing insight into the relationships between the anatomical and/or physiological properties of the fiber and the shape of the potential.

6.2 Impact on teaching and learning

Although the convolutional model presented in equations from (1) to (7) has low complexity, students often found difficulties when trying to interpret such equations. In fact, from data gathered during three years of teaching this subject, approximately 30% of the students showed problems when they were asked to explain the possible effects of change in some of the model's parameters. The main goal of the simulation programs implemented in MATLAB was to provide students with a comprehensive set of

training and learning functions to improve the understanding of the electrical activity generated by the excitable muscle fiber. Such programs allow the students to reflect on the different aspects involved in the study of biological phenomena:

- Identify the anatomical, physiological and functional properties of the motor unit.
- Integrate the abovementioned properties into a convolutional model that comprises the three spatial dimensions.
- Distinguish the role of the excitation source of the system from that of its impulse response.
- Analyze the effect of the recording conditions (electrode position) on the features of extracellular potentials.
- Predict the effects of change in the physiological features of the fiber (fiber diameter, conduction velocity) on the features of extracellular potentials.
- Integrate the inherent variability associated to the motor unit parameters into the model through statistical distributions.

During the last week of the semester, students were asked to comment on the problems they faced in this course. A number of suggestions were made. Several features have been taken into account:

- Students were asked to use the simulation programs of MATLAB (see Appendix) to answer a number of questions related to the amplitude- and time-related characteristics of extracellular potentials. By using the default values shown in Tables 1 and 2, they developed a good understanding of the generation of electrical potentials and their dependence on the recording conditions and on the physiological and functional properties of muscle fibers.
- Students had the opportunity to gain insight into the concept of convolution and to reflect on its usefulness to model biological systems. Most students (86% of the total) understood the rationale for using an excitation source to model the intracellular potential that travels along the fiber and an impulse response that comprises the geometrical and physiological properties of the fiber. The simulation programs offered the students the possibility of displaying the time course of each of these signals separately. Those students who showed difficulties in understanding the concept of convolution (14%) could improve their comprehension by observing such signals.
- By analyzing the simulation programs, students were given a good platform on which they can learn how to write their own optimized functions. From the feedback, students benefited most by working with these efficient programming templates. The programs were subjected to changes, allowing advanced students to test their own algorithms, therefore gaining extra bonus marks.
- Evidence from the feedback demonstrates that

most students expressed their strong support and keenness in working with these models and programs. Those students who had a lack of knowledge on programming on MATLAB (23% of the total) had the opportunity to learn the basic commands and functions as the code was clear and intuitive, whereas those with more programming experience (77%) further developed their skills.

8. CONCLUSIONS

The objective of this paper is to provide biomedical engineering students with an example of modelling and computer simulation of the electrical behaviour of the motor unit. A theoretical basis of the extracellular electrical potential produced by an excitable fiber was presented starting with the basic equations and including the anatomical and physiological parameters. Such extracellular potential was modelled as the convolution between an excitation source and an impulse response. Despite the simplicity of this mathematical formulation, students are often not able to interpret correctly the equations and to develop an intuition about the role of the underlying physiological parameters (30% of the total). Our teaching experience reveals that a comprehensive set of simulation programs is always necessary for the students to obtain a deeper understanding of the bioelectrical phenomena behind the equations.

By using a set of simulation programs, based on the convolutional model, the students can feel the effects of changes in the detection conditions and fibers' physiological properties on the characteristics of the electrical potential. The programs also allow the students to separate the role of the excitation source from that of the impulse response in the generation of the potential, therefore gaining insight into the concept of convolution. The authors have noticed that the ability to display the time course of the different signals is especially useful as it allows the students to match the analytical expression of the signals with their corresponding physical appearance.

Our experience has shown that these simulation programs and methodology have clearly heightened student interest in the learning of electrical models of the muscle and Electromyography. Indeed, the simulation programs were used by the students as a platform on which they can gain confidence before attempting to develop their own algorithms. It is the desire of the authors to integrate the model presented here within an interactive application in order to help students to obtain a better comprehension of the generation of extracellular potentials.

Acknowledgement—This work was supported by the Spanish Ministry of Education & Science under the project SAF2007-65383.

REFERENCES

1. Anonymous, Definition of biomedical engineering, The Whitaker Foundation, Available online: <http://bmes.org/WhitakerArchives/glance/definition.html>
2. L. D. Harmon, Biomedical engineering education: how to do what, with which, and to whom, *IEEE Transactions on Biomedical Engineering*, **22**(2), 1975, pp. 89–94.
3. R. J. Johns, Current issues in biomedical engineering education, *IEEE Transactions on Biomedical Engineering*, **22**(2), 1975, pp. 107–110.
4. H. R. Weed, Biomedical engineering-practice or research? *IEEE Transactions on Biomedical Engineering*, **22**(2), 1975, pp. 110–114.
5. K. C. Mylrea and S. E. Sivertson, Biomedical engineering in healthcare-potential versus reality, *IEEE Transactions on Biomedical Engineering*, **22**(2), 1975, pp. 114–119.
6. A. R. Kahn, Biomedical engineering education for employment by industry, *IEEE Transactions on Biomedical Engineering*, **22**(2), 1975, pp. 147–149.
7. A. R. Potvin, F. M. Long, J. G. Webster, and R. J. Jendrucko, Biomedical engineering education: enrollment, courses, degrees, and employment, *IEEE Transactions on Biomedical Engineering*, **28**(1), 1981, pp. 22–28.
8. T. C. Pilkington, F. M. Long, R. Plonsey, J. G. Webster, and W. Welkowitz, Status and trends in biomedical engineering education, *IEEE Engineering in Medicine and Biology Magazine*, 1989, pp. 9–17.
9. J. G. Webster, Guest editorial, *International Journal of Engineering Education*, **15**(4), 1999, pp. 238–239.
10. P. King, Design and biomedical engineering, *International Journal of Engineering Education*, **15**(4), 1999, pp. 282–287.
11. J. Viik and J. Malmivuo, Biomedical engineering as a career resource: survey from Tampere University of Technology, *International Journal of Engineering Education*, **15**(4), 1999, pp. 308–320.
12. J. Bronzino, Biomedical engineering: a historical perspective, in J. Enderle, S. Blanchard, and J. Bronzino (Eds) *Introduction to Biomedical Engineering*, 2nd edn, USA: Academic Press, San Diego, CA, 2005, pp. 1–29.
13. Z. O. Abu-Faraj, Bioengineering/Biomedical Engineering Education and Career Development: Literature Review, Definitions, and Constructive Recommendations, *International Journal of Engineering Education*, **24** 2008, pp. 990–1011.
14. The Whitaker Foundation Biomedical Engineering Education Summit Meetings. Available online: <http://www.bmes.org/WhitakerArchives/summit/index.html>.
15. J. Malmivuo, and R. Plonsey, *Bioelectromagnetism: Principles and Applications of Bioelectric and Biomagnetic Fields*, Oxford University Press, Oxford, 1995.
16. R. E. Burke, Motor units: anatomy, physiology and functional organization. In: Handbook of Physiology. The Nervous System. Motor Control. Bethesda, MD: *American Physiological Society*, **2**, 1981, pp. 345–422.
17. F. Buchthal, F. Erminio, P. Rosenfalck, Motor unit territory in different human muscles, *Acta Physiologica Scandinavica*, **45** 1959, pp. 72–87.
18. D. S. Cordray, G. M. Pion, A. Harris, and P. Norris, The value of the VaNTH Engineering Research Center, *IEEE Engineering in Medicine and Biology Magazine*, **22**(4), 2003, pp. 47–54.
19. Anonymous, Criteria for accrediting engineering programs-effective for evaluations during the 2008–2009 accreditation cycle, *Engineering Accreditation Commission, ABET, Inc.* Baltimore, MD, USA, pp. 19.
20. J. R. Daube, D. I. Rubin, Needle electromyography, *Muscle Nerve*, **39**, 2009, pp. 244–270.
21. R. Lorente de Nó, *Analysis of the distribution of action currents of nerve in volume conductors*, Studies from the Rockefeller Institute for Medical Research, **132**, 1947, pp. 384–485.
22. R. Plonsey, The active fiber in a volume conductor. *IEEE Transactions on Biomedical Engineering*, **21**, 1974, pp. 371–381.
23. R. Plonsey, Action potential sources and their volume conductor fields, *Proceedings IEEE*, **65**, 1977, pp. 601–611.
24. S. Andreassen, A. Rosenfalck, Relationship of intracellular and extracellular action potentials of skeletal muscle fibers, *CRC Critical Reviews in Bioengineering*, **7**, 1981, pp. 267–306.
25. B. A. Albers, W. L. C. Rutten, W. Wallinga-de Jonge, and H. B. K. Boom, Microscopic and macroscopic volume conduction in skeletal muscle tissue, applied to simulation of single fiber action potentials, *Medical and Biological Engineering and Computing*, **26**, 1988, pp. 605–610.
26. G. V. Dimitrov, N. A. Dimitrova, Precise and fast calculation of the motor unit potentials detected by a point and rectangular plate electrode, *Medical Engineering & Physics*, **20**, 1998, pp. 374–381.
27. S. Nandedkar, E. Stålberg, Simulation of single muscle fiber action potentials, *Medical and Biological Engineering and Computing*, **21**, 1983, pp. 158–165.
28. J. Tung, MATLAB and Simulink in Engineering Education, *International Journal of Engineering Education*, **21**, 2005, pp. 560.
29. J. Z. Zhang, R. Adams and K. Burbank, Theory, Practice and Systems- A new Approach to Teaching Electronic Communications with MATLAB, *International Journal of Engineering Education*, **21**, 2005, pp. 612–617.
30. E. D. Ubeyli and I. Guler, Teaching Automated Diagnostic Systems for Doppler Ultra Sound Blood Flow Signals to Biomedical Engineering Students using MATLAB, *International Journal of Engineering Education*, **21**, 2005, pp. 649–667.
31. F. Buchthal, The functional organization of the motor unit: a summary of results, *American Journal of Physical Medicine*, **38**, 1959, pp. 125–8.
32. R. L. Lieber, *Skeletal Muscle Structure and Function: Implications for Rehabilitation and Sports Medicine*, Williams & Wilkins. Maryland, USA, 1992, pp. 34–35.

33. E. Stålberg, Propagation velocity in human muscle fibers in situ, *Acta Physiologica Scandinavica*, **287**, 1966. pp. 1–112.
34. N. Dimitrova, Mathematical modelling of intra- and extracellular potentials generated by active structures: effects of a step change in structure diameter, *General Physiology and Biophysics*, **6**, 1987, pp. 19–34.
35. S. S. Goldstein and W. Rall, Changes of action potential shape and velocity for changing core-conductor geometry, *Biophysical Journal*, **14**, 1974, pp. 731–757.
36. J. Rodríguez, A. Malanda, L. Gila, I. Rodríguez, J. Navallas, A mathematical analysis of SFAP convolutional models, *IEEE Transactions on Biomedical Engineering*, **52**(5), 2005, pp. 769–783.
37. N. A. Dimitrova, G. V. Dimitrov, Amplitude-related characteristics of motor unit and M-wave potentials during fatigue. A simulation study using literature data on intracellular potential changes found in vitro, *Journal of Electromyography and Kinesiology*, **12**, 2002, pp. 339–349.
38. D. W. Stashuk, Simulation of electromyographic signals, *Journal of Electromyography and Kinesiology*, **3**, 1993, pp. 153–173.
39. V. M. Bernsteyn, Modelling of electric signal of muscle fibers group. *Biophysika*, **12**, 1967, pp. 1059–63.
40. C. E. T. Krakau, A note on the Fourier Transform of Lorente de No's potential function of the external field of a nerve in a volume conductor, *Kgl. Fysiogr. Sallsk.*, **27**, 1957, pp. 177–83.

APPENDIX (MATLAB code)

```
function [y,exc,IR,t]= sfap();
%%%%%%%%%%%%%%%%%%%%%%%%%%%%%%%%%%%%%%%%%%%%%%%%%%%%%%%%%%%%%%%%%%%%%%%%
% sfap function calculates the extracellular potential generated by the
% propagation of the transmembrane potential along the fibre and recorded
% a detection point. The fibre is considered as a time-shift invariant system
% and so the sfap is calculated as the convolution of an input signal and a impulse response
%
% [y,exc,IR,t]= sfap
% y: single fibre action potential (sfap) in the temporal domain
% exc: excitation function (transmembrane potential second derivative)
% IR: impulse response
% t: sampling interval of the sfap
%
% Model parameters:
% L1: right semilength (distance from the neuromuscular junction to the right fibre end) (L1.ref=40 mm)
% L2: right semilength (distance from the neuromuscular junction to the left fibre end) (L2.ref=50 mm)
% z0: longitudinal distance of the electrode (z-axis) (z0.ref: 20 mm)
% nmj: Position of the neuromuscular junction with respect to the coordinate origin
% r: radial distance of the electrode (r.ref: 0.1 mm)
% diam: fibre diameter (v.ref: 0.055 mm)
% cv: muscle fibre conduction velocity (cv.ref: 4 m/s = 4 mm/ms)
% dt: sampling interval of signals (dt.ref: 0.01 ms)
% Tmax: maximum duration of the membrane potential (Tmax.ref: 4 ms)
%
% Author: Javier Rodr guez, 2007.
%%%%%%%%%%%%%%%%%%%%%%%%%%%%%%%%%%%%%%%%%%%%%%%%%%%%%%%%%%%%%%%%%%%%%%%%

%Parameters:
L1= 40;
L2= 50;
z0= 20;
nmj=0;
r= 0.1;
diam=0.055;
dt= 0.025;
Tmax= 4;
k1= 0.02;

% Calculation of the excitation function:
[vm,t_exc]= iap(diam,dt,Tmax);
d_vm= deriv(vm,dt);
exc= deriv(d_vm,dt);
```

```

% Calculation of the impulse response:
[IR,t_IR]= IR_system(L1,L2,z0,nmj,r,diam,dt);

% Final convolution to obtain the sfap:
y= -k1*diam.^2*conv(exc,IR);

% Plotting of the signals:
figure, plot(t_IR,IR), grid;
title('Impulse response');
xlabel('Time (ms)');

figure, plot(t_exc,exc), grid;
title('Excitation function (2nd derivative of vm)');
xlabel('Time (ms)');

tlimit= dt*(length(y)-1);
t=0:dt:tlimit;
figure, plot(t,y), grid;
title('Extracellular potential recorded from one fibre (sfap)');
xlabel('Time (ms)');

function y=deriv(x,dt);
%%%%%%%%%%%%%%%%%%%%%%%%%%%%%%%%%%%%%%%%%%%%%%%%%%%%%%%%%%%%%%%%%%%%%%%%
% deriv function calculates the first order approximation of a signal first derivative in discrete domain
%
% x: input signal
% dt: sampling interval (dt.ref: 0.01 ms)
% y: output signal (derivative of x)
%
% Author: Javier Rodr guez, 2007.
%%%%%%%%%%%%%%%%%%%%%%%%%%%%%%%%%%%%%%%%%%%%%%%%%%%%%%%%%%%%%%%%%%%%%%%%

y=filter([1,-1],1,x)/dt;

function [vm,t]= iap(diam,dt,Tmax);
%%%%%%%%%%%%%%%%%%%%%%%%%%%%%%%%%%%%%%%%%%%%%%%%%%%%%%%%%%%%%%%%%%%%%%%%
% Iap function calculates the membrane potential of a muscle fibre
% Default values: [vm,t]= iap(4,0.01,4)
%
% Input parameters:
% diam: fibre diameter (v.ref: 0.055 mm)
% dt: sampling interval of signals (dt.ref: 0.01 ms)
% Tmax: maximum duration of the membrane potential (Tmax.ref: 4 ms)
%
% Output parameters:
% vm: membrane potential
% t: vector with the time axis
%
% Author: Javier Rodr guez, 2007.
%%%%%%%%%%%%%%%%%%%%%%%%%%%%%%%%%%%%%%%%%%%%%%%%%%%%%%%%%%%%%%%%%%%%%%%%

cv= 4 + 0.05*(diam-0.055); % calculation of the conduction velocity using
                           % the fibre diameter (cv.ref: 4 m/s = 4 mm/ms)

t=0:dt:Tmax;
z= cv*t;
vm= 96*(z.^3).*exp(-2*z);

function [IR,t]= IR_system(L1,L2,z0,nmj,r,diam,dt);
%%%%%%%%%%%%%%%%%%%%%%%%%%%%%%%%%%%%%%%%%%%%%%%%%%%%%%%%%%%%%%%%%%%%%%%%
% IR_system function calculates the impulse response of the time-shift invariant system
% The IR represents the potential produced at a detection point by two current monopoles
% propagating along the fibre in opposite directions from the endplate toward the fibre ends

```

```

%
% Default values: IR= IR_system(40,50,20,0.2,4,0.063,0.01)
%
% Input parameters:
% L1: right semilength (distance from the neuromuscular junction to the right fibre end) (L1.ref=40 mm)
% L2: right semilength (distance from the neuromuscular junction to the left fibre end) (L2.ref=50 mm)
% z0: longitudinal distance of the electrode (z-axis) (z0.ref: 20 mm)
% nmj: Position of the neuromuscular junction with respect to the coordinate origin
% r: radial distance of the electrode (r.ref: 0.1 mm)
% diam: fibre diameter (diam.ref: 0.0579 mm)
% dt: sampling interval of signals (dt.ref: 0.01 ms)
%
% Output parameters:
% IR: impulse response
% t: vector with the time axis
%
% references: R. Plonsey, C. Barr, "Bioelectricity. A quantitative approach". Plenum Press, 1998.
%
% Author: Javier Rodr guez, 2007.
%%%%%%%%%%%%%%%%%%%%%%%%%%%%%%%%%%%%%%%%%%%%%%%%%%%%%%%%%%%%%%%%%%%%%%%%

cv= 4 + 0.05*(diam-0.055); % calculation of the conduction velocity using
                           % the fibre diameter (cv.ref: 4 m/s = 4 mm/ms)
tmax= max(L1,L2)/cv;      % IR duration
N= floor(tmax/dt) + 1;    % IR duration in samples
t= 0: dt: dt*(N-1);      % vector with the time axis

T1= L1/cv;                % Time for the right excitation to reach the right end of the fibre
N1= floor(T1/dt);        % T1 measured in samples

T2= L2/cv;                % Time for the left excitation to reach the left end of the fibre
N2= floor(T2/dt);        % T1 measured in samples

N_min= min(N1,N2);       % if the two excitations are travelling
for n=1: N_min + 1
    r1= ((z0-nmj-cv*t(n)).^2 + r^2)^0.5;
    r2= ((z0-nmj+cv*t(n)).^2 + r^2)^0.5;
    IR(n)= 1/r1 + 1/r2;
end

if N1>N2                  % if only the right excitation is travelling
    for n= N_min + 2: N
        r1= ((z0-nmj-cv*t(n)).^2 + r^2)^0.5;
        IR(n)= 1/r1;
    end
else                      % if only the left excitation is travelling
    for n= N_min + 2: N
        r2= ((z0-nmj+cv*t(n)).^2 + r^2)^0.5;
        IR(n)= 1/r2;
    end
end
end

```

Javier Rodr guez graduated from the Public University of Navarra, Spain in 2003. He obtained the Ph.D. degree in 2007 from the Public University of Navarra, Telecommunication Engineering. He worked as a Consultant Engineer (2004-2005) and as a System Engineer (2005-2006) in the private sector. He has also worked for the Higher Scientific Investigation Council of Spain during one year (2006). In 2007 he became Assistant Professor in the Electrical and Electronics Engineering Department of the Public University of Navarra. During this period he has been teaching several subjects related to digital signal processing, image processing and biomedical engineering. His research focuses on signal processing applied to biomedical signals, modeling of biological systems, electromyography and sensory-motor interaction studies.

Armando Malanda graduated from the Madrid Polytechnic University, Spain in 1992. He obtained the Ph.D. degree in 1999 from the Carlos III University, Madrid, Telecommunication Engineering. In 1992 he joined the School of Telecommunication and Industrial Engineering of the Public University of Navarra. In 2003 he became Associate Professor in the Electrical and Electronics Engineering Department of this University. Since 1992, he has been teaching several subjects related to digital signal processing, image processing and biomedical engineering. His areas of interest comprise the analysis, modeling and simulation of bioelectrical signals, particularly EEG and EMG.

Javier Navallas graduated from the Public University of Navarra, Spain in 2002. He obtained the Ph.D. degree in 2008 from the Public University of Navarra, Telecommunication Engineering. He has also worked as a software engineer. He is presently Assistant Professor in the Electrical and Electronics Engineering Department of this University. His research interests are modeling of biological systems and neurosciences.